Version of Record: https://www.sciencedirect.com/science/article/pii/S0039914023001108
Manuscript_e47abfac93008fb9a2045b4742c021d5

Dual detection chromatographic method for fast characterization of nano-gravimetric detector

Michel RACHKIDI [a, b, *], Laura ALONSO-SOBRADO [a], Guy RAFFIN [b], Eric COLINET [a], Jérôme RANDON [b]

[a] APIX Analytics, 38000 Grenoble, France

[b] Université de Lyon, CNRS, Université Claude Bernard Lyon 1, Institut des Sciences Analytiques, UMR 5280, F-69100 Villeurbanne

* Corresponding author.
E-mail address: michel.rachkidi@apixanalytics.com

Abstract

Nano-gravimetric detector (NGD) has been recently introduced as miniaturized gas chromatography detector. The NGD response is based on an adsorption-desorption mechanism of compounds between the gaseous phase and the NGD porous oxide layer. The NGD response was characterized by hyphenating NGD in-line with FID detector and a chromatographic column. Such method led to the full adsorption-desorption isotherms of several compounds in a single run. Langmuir model was used to describe the experimental isotherms, and the initial slope of the isotherm ($Mm.K_T$) obtained at low gas concentration was used to compare the NGD response for different compounds (good repeatability was demonstrated with a relative standard deviation lower than 3%). The column-NGD-FID hyphenated method was validated using alkane compounds according to the number of carbon atoms in the alkyl chain and to the NGD temperature (all results agreed with thermodynamic relations associated to partition coefficient). Furthermore, relative response factor to alkanes, for ketones, alkylbenzenes, and fatty acid methyl esters have been obtained. These relative response index values led to easier calibration of NGD. The established methodology can be used for any sensor characterization based on adsorption mechanism.

Keywords:

Gas analysis

Nano-gravimetric detector

Adsorption-desorption isotherms

Chromatography

1. Introduction

Quantification of air quality is becoming more and more important in the context of environment monitoring, human health, or manufacturing of products and formulations [1–3]. In this context, the development and production of gas microsensors has increased during the last decade. Interactions between a microsensor-sensitive layer and a specific analyte can lead to a change in electrophysical properties of sensors (resistance, electrical permittivity, resonance frequency…) in relation to the quantity of the analyte in the sample [4]. Some microsensors are dedicated to specific analytes (highly specific) and cannot simultaneously quantify several compounds in a complex mixture. Other sensors are non-specific and can detect a large variety of molecules. Usually they are used with a gas chromatography system (GC) that ensures the separation of gases initially mixed in the sample before detection and quantification by the sensor itself [5–7]. In such GC configuration, sensors with low time constant are mandatory to avoid loss of separation efficiency. The main advantage of gas microsensors as detectors in a GC is related to their small footprint and non-destructive nature, which paves the way to system miniaturization and multiplexing [8,9].

Recently, a nano-gravimetric detector based on nano-electromechanical systems (NEMS) technology has been proposed [10]. This detector is universal and the rapid exchange kinetics on the detector surface are compatible with high-speed analyzes in gas chromatography. In short, the NGD consists of an array of identical silicon nanobeams (25 beams, each beam: 5 µm long, 300 nm wide and 160 nm thick) covered by chemical vapor deposition with a 180 nm thick porous oxide layer. This coating allows the adsorption-desorption of various gaseous compounds at the surface of the nanobeams. Each beam has a defined mass (M_{eff}) and so has a specific resonance frequency (f_0) which can be measured thanks to a phase-locked-loop (PLL) electronic circuitry. A mass shift (m_{ads}) caused by the adsorption-desorption of molecules on the surface of the beam leads to a proportional shift of the

resonance frequency of the beam. So, the detector response R(t) is a continuous measurement of the resonance frequency variation (Δf) and was described with Eq. (1):

$$R(t) = \Delta f(t) = \left(\frac{f_0}{2M_{eff}}\right).m_{ads}(t) \quad (1)$$

Due to the adsorption-desorption mechanism of this detection system, the sensitivity of the NGD is directly related to the partition equilibrium of the compound between the gaseous phase and the adsorbent material deposited on the beam. However, a plot of analyte peak area versus analyte concentrations shows that the NGD response is not linear for high concentrations. This nonlinear response makes the quantification of compounds much more difficult and thus, a more suited response model has to be introduced allowing an optimal fit of the data associated to the adsorption-desorption isotherm of the analyte on the detector surface.

Usually, to obtain the data set required to represent the isotherm of a single analyte on an adsorbent, a constant carrier gas flow is first introduced at a controlled temperature into the sensor cell. The targeted analyte, diluted in the carrier gas at the desired concentration, is then delivered to the sensor until equilibrium is reached (in accordance with the response time of the sensor) [11–13]. To build a complete isotherm, such method appears to be time consuming because each experiment only allows the characterization of one single analyte at one specific concentration. So, several experiments must be performed to obtain the full isotherm for only one single analyte.

Therefore, we introduced a reliable fast method to characterize the adsorption process (full adsorption-desorption isotherm) between a gas sensor surface and several compounds in a single run. For this purpose, the NGD detector has been setup in-line in a conventional lab GC: column - NGD - Flame Ionization Detector (FID). In the past, such hyphenation has been applied with other gas sensors, mainly to compare sensitivity and LOD [14–16]. When adsorption process has been investigated using such configuration [8,10], constant partition coefficients (K_T) were assumed. Such assumption is probably valid when low amount of analyte is introduced in the column, but in our

previous work [10], we also observed a deviation from linearity (peak area – injected quantity) when the analyte concentration increased. Such deviation could be linked to non-linear adsorption isotherms, and so isotherms have to be determined for more accurate quantification in a broader range of analyte concentration. Here, we processed data from NGD and FID detectors to obtain complete sorption isotherms of several compounds using only one chromatographic run. During a chromatographic run, the concentration profile of an analyte in the mobile phase C_m (t) varies over time and was monitored using the FID signal. Simultaneously, the adsorbed mass of analyte on the surface of the beams m_{ads} (t) was tracked using the NGD signal. These two data sets were then linked to plot adsorption isotherm.

2. Material and methods

2.1. Reagents and standards

Different standards of alkanes, alkylbenzenes, ketones, and esters were used. Alkanes (pentane, hexane, heptane, octane, nonane, decane, undecane, tridecane, tetradecane, pentadecane, hexadecane, heptadecane, octadecane, nonadecane), alkylbenzenes (Benzene, ethylbenzene, propylbenzene, butylbenzene, pentylbenzene, hexylbenzene) and ketones (pentan-2-one, hexan-2-one, heptan-2-one, octan-2-one, nonan-2-one, decan-2-one) were purchased from Sigma-Aldrich (France). Esters (methyl octanoate, methyl nonanoate, methyl decanoate, methyl undecanoate, methyl dodecanoate) were obtained from Thermo Scientific (France). Several compound mixtures were prepared in pentane at 10 $g.L^{-1}$.

2.2. GC-NGD-FID instrument

As shown in Fig. 1, a Clarus® 500 Gas Chromatograph (Perkin-Elmer, France) with an automatic sampler, split/spitless injector, and a flame ionization detector with a fused silica DB-5MS capillary column (15 m length, 250 µm internal diameter, 0.1 µm film thickness, Agilent France) was used. The

NGD (model NANOPIX from APIX Analytics SA, Grenoble, France) is plugged on the top side of the GC instrument. The inlet and outlet of the NGD are connected to the GC column and to the FID through a heated transfer line, which is a 20 cm long stainless-steel tubing with an internal diameter of 250 µm. The connections to the transfer line are done via a universal press-tight connector with a 60/40 Vespel/Graphite Compact Capillary Ferrules of 0.4 mm internal diameter. The transfer line temperature was maintained at 200°C during all experiments to prevent condensation without affecting the NGD temperature which can be controlled from 70 to 200°C. A deactivated fused silica capillary with an internal diameter of 200 µm connects the transfer line to the FID. The injector port and FID temperatures were fixed at 250°C. For liquid injection, 1 µL of sample was injected into the injector in split mode (split ratio ≈ 25) using a 5 µL syringe from Perkin-Elmer Helium was used as the carrier gas at constant pressure of 1 bar. The FID was operated with an airflow of 450 mL min^{-1} and hydrogen flow of 45 mL min^{-1}. Regeneration of the NGD detector was systematically carried out between analyses by maintaining NGD temperature at 200°C for 2 min.

2.3. Data treatment

Two signals were recorded during chromatographic run: NGD signal and FID signal. Signal processing and treatment were then carried out and consist of : (1) Resample the signals with the same sampling period (δt = 0.001min) as the FID and NGD acquisition frequencies were not the same; (2) Realign the FID signal according to the NGD hold-up time peak in order to correct the time delay between the two detectors; (3) Suppress the baseline by eliminating the offset and drift; (4) Convert FID and NGD values to mobile phase concentration C_m and adsorbed mass on the beam m_{ads}; (5) Plot isotherms $m_{ads}=f(C_m)$.

The total quantity of matter of analyte injected in the column (n_t) depends on the injected concentration (C_{inj}), injected volume (V_{inj}) and split ratio (SR). On the FID chromatogram Y(t), this injected amount is represented by the peak area and associated to the FID sensitivity (S) according to Eq. (2):

$$n_t = \frac{C_{inj} \cdot V_{inj}}{SR} = \frac{\int Y(t) \cdot dt}{S} \quad (2)$$

In the time interval δt between two measurements, a fraction of this injected amount (δn) has gone through the FID detector and this amount can be calculated based on a fraction of the peak area observed with the FID according to Eq. (3):

$$\delta n = n_t \frac{Y(t) \cdot \delta t}{\int Y(t) \cdot dt} \quad (3)$$

In the time interval δt, the volume of gas δv through the FID detector can be estimated using column flow (F) and Eq. (4):

$$\delta v = F \cdot \delta t \quad (4)$$

So the mobile phase concentration C_m (t) was calculated using Eq. (5):

$$C_m(t) = \frac{\delta n}{\delta v} \quad (5)$$

All these relations were combined in Eq. (6):

$$C_m(t) = \frac{C_{inj} \cdot V_{inj}}{SR} \cdot \frac{Y(t)}{\int Y(t) \cdot dt} \cdot \frac{1}{F} \quad (6)$$

By calculating m_{ads} using Eq. (1) and C_m using Eq. (6), it is possible to plot the isotherm of different compounds through a single chromatographic run.

3. Results and Discussion

3.1. Isotherm construction

GC-NGD-FID instrument generates two chromatograms: the FID chromatogram linked to the gas phase concentration C_m, and the NGD chromatogram linked to the absorbed mass m_{ads} on the beam surface. Both FID and NGD chromatograms have been combined to characterize the adsorption

process on the beam surface. In this configuration, the GC system played the role of a gas generator. Optimal chromatographic conditions were purposely avoided by overloading the separation column, as the objective of the study was not to investigate the separation column efficiency nor the interaction between the mobile phase and column stationary phase. Column overload allowed a quasi-linear increase of the concentration in the mobile phase through time, compared to a Gaussian peak with sharper variations. Thus, it was more convenient to determine accurately and simultaneously $C_m(t)$ and $m_{ads}(t)$, and so the full isotherm during the analyte elution.

To illustrate the data processing method, a mixture of alkanes from decane (C_{10}) to tetradecane (C_{14}) in pentane (C_5) at 10 $g.L^{-1}$ was injected in isothermal conditions (T_{oven} = 110°C and T_{NGD} = 130°C) and chromatograms are presented in Fig. 2(A). Detectors signals have been normalized to the highest value in each chromatogram for easier comparison, and normalized data have been plotted for C_{14} in Fig. 2(B). For each specific time (a vertical line going through both signals in Fig. 2(B)), the NGD signal (top chromatogram in Fig. 2(B)) allows us to calculate m_{ads} using Eq. (1) and the corresponding point of the FID signal (bottom chromatogram in Fig. 2(B)) allows us to calculate C_m according to Eq. (6). This calculation has been performed for each time value with a fixe time interval (δt = 0.001 min). From all (m_{ads}, C_m) values, the experimental isotherm was plotted in Fig. 2(C).

Langmuir model [17] was used to describe isotherm data. For an analyte A, with adsorption sites of equal binding energy, the fractional occupancy of the adsorption sites θ_A is related to the thermodynamic equilibrium constant (K) and to the gas partial pressure (P_A) according to Eq. (8):

$$\theta_A = \frac{P_A \,.\, K}{P_A \,.\, K + 1} \quad (8)$$

Furthermore, the partial pressure P_A is proportional to the mobile phase concentration C_m, and the fractional occupancy of the adsorption sites θ_A is the ratio of the adsorbed quantity (m_{ads}) to the mass of gas molecules monolayer covering the whole surface of the beam (Mm). Based on these assumptions, Eq. (9) can be used to link all these parameters:

$$m_{ads}(t) = Mm \cdot \frac{C_m(t).K_T}{C_m(t).K_T + 1} \quad (9)$$

When this model was applied to fit the experimental isotherm data points, good correlation was obtained as illustrated in Fig. 2(C) for the analyte concentration range used. It should be mentioned that using solutions with much higher concentration of alkanes (unreported experiments), the isotherm for higher $C_m(t)$ values led to a shape similar to the one observed in a multilayer model. However, to be realistic compared to the analyte concentration in conventional samples, the monolayer model was relevant enough to describe the experimental data. In such conditions, because adsorption was far from saturation, Mm and K_T cannot be independently determined in a very accurate way. However, the sensitivity ($Mm.K_T$) can be precisely quantified (RSD<3%) and used further to compare the NGD response for different compounds under various conditions.

3.2. Carbon number effect

As observed in the chromatograms of C_{10} to C_{14} (Fig. 2(A)), FID peak height decreased from C_{10} to C_{14} while peak area stayed constant as expected for a mass-flow dependent detector. On the other side, the NGD peak height and peak area increased from C_{10} to C_{14} suggesting that the NGD sensitivity is strongly dependent on the solute. Therefore, several experiments were performed using three different alkane solutions: C_6 to C_{10}, C_{10} to C_{14}, and C_{14} to C_{19} in C_5 at 10 $g.L^{-1}$ each (injected quantity was approximatively 400 ng for each compound). These mixtures were analyzed in isothermal conditions (T_{oven} = 60, 110 and 140°C respectively for optimal separation conditions) at a constant NGD temperature of 130°C. Alkane isotherms are displayed in Fig. 3(A) for C_{10} to C_{14}.

For the same mobile phase concentration, the amount adsorbed on the NGD surface increased from C_{10} to C_{14}, which is translated by an increase of the initial slope. As presented in Fig. 3(B), logarithm of the sensitivity increases linearly as a function of number of carbon atoms in the alkyl chain.

The NGD sensitivity for a specific compound can be related to the logarithm of the slope at the origin of the isotherms, characterized by Ln ($Mm.K_T$), and this value increases regularly with each CH_2

addition into the alkane chain. Each thermodynamic equilibrium related to one specific compound is characterized by an enthalpy change $\Delta_r H$, and $\Delta\Delta_r H$ is constant over the range from C_7 to C_{19} (Fig. 3(B)). Such type of phenomenon is also observed for chromatographic separation (Fig. 2(A)) which is also based on phase partitioning between stationary and mobile phase. In chromatographic separation, the logarithm of the alkane retention factor ($k=t_R/t_m-1$ with t_R retention time, t_m hold-up time) varies linearly with the number of carbon atoms in the alkane chain, i.e. the retention time of alkane varies exponentially as illustrated in Fig. 2(A).

3.3. Temperature effect

To study the temperature effect, alkane mixture of C_{10} to C_{14} in C_5 at 10 $g.L^{-1}$ was analyzed in isothermal conditions (T_{oven} = 110°C), at different NGD temperatures from 70 to 150°C. Fig. 4 displays C_{14} chromatograms and associated isotherms observed at different NGD temperatures. The slight increase in retention time of C_{14} peak with the detector temperature is due to the increase of gas viscosity in the NGD detector leading to an increased flow resistance in the detector cell. As expected, FID peak area did not change as the injected quantity was the same whatever the NGD detector temperature (relative standard deviation of C_{14} FID peak area = 2.2%). On the other side, the NGD peak area decreased as the NGD temperature increased. This observation is highlighted in the isotherms with a decrease of the absorbed amount at higher NGD temperature for a fixed gas phase concentration. These observations are related to the partition coefficient K_T which is only dependent on temperature. Standard enthalpy ΔH° and standard entropy ΔS° of adsorption are assumed to be constant according to Ellingham approximation and Eq. (10) can be used to describe the temperature dependence of the adsorption-desorption process.

$$\mathrm{Ln}\,(K_T) = -\frac{\Delta H^\circ}{RT} + \frac{\Delta S^\circ}{R} \quad (10)$$

where R is the gas constant and T is the NGD absolute temperature.

The logarithm of the NGD sensitivity (Ln ($Mm.K_T$)) obtained from C_{10} to C_{14} isotherms has been plotted versus 1/T for each compound (Fig. 5): linear trends are observed according to thermodynamic relationship (Eq. (10)). As previously reported, the slope Δ_rH/R increases linearly as a function of the number of carbon atoms in the alkly chain ($\Delta CH_2 = \Delta\Delta_rH$).

With all these information, it is then possible to predict the NGD sensitivity for linear alkane molecule at any given temperature.

3.4. Relative response for different compounds

The isotherms for different families such as alkylbenzenes (from benzene to hexylbenzene), ketones (from pentan-2-one to decan-2-one), and methyl esters (from methyl octanoate to methyl dodecanoate) have been studied. Experiments were conducted with mixtures of different compounds form the same family, at a constant NGD temperature, and NGD sensitivity was determined from the isotherms. Fig. 6 shows the response for the different families of compounds as a function of the number of carbon atoms in the molecular structure at T_{NGD} = 130°C.

For the same number of carbon atoms, a higher response means a greater affinity of the compound with the silicon porous oxide covering the resonator beam. As an example, for compounds with 10 atoms of carbon, the affinity increases as follow: decane < butylbenzene < decane-2-one ≈ methyl nonanoate. This is in accordance with the polar nature of the compounds that allow stronger interactions with the silicon porous oxide layer.

For a specific compound (such as decan-2-one as an example, Fig. 6, x-axis: 10 carbon atoms), the logarithm of sensitivity (4.40) lies between two adjacent hydrocarbons (tridecane 4.08 and tetradecane 4.95). Based on this observation, it is possible to define a sensitivity scale in relation to linear alkanes (nC_{alkane}). In our example, decan-2-one response is similar to a hypothetic alkane with a

number of carbon atoms of 13.08. So we can define the relative response index (I_R) as the hypothetical number of carbon atoms multiplied by 100, which is therefore 1308 for decan-2-one.

This method takes advantage of the linear relationship between the values of Ln ($Mm.K_T$) and the number of carbon atoms in a hydrocarbon chain and this index is useful to convert NGD response to system-independent constants. The same way that the Kovats index compares the retention of a specific compound to the alkanes on a GC column with a specific stationary phase, the relative response Index compares the NGD sensitivity to the alkanes.

The simplest way to calculate the relative response Index is to interpolate the NGD sensitivity of a compound between the sensitivity for adjacent n-alkanes (Eq. (11)).

$$I_R = 100 \times [\, n + \frac{R_x - R_n}{R_{n+1} - R_n} \,] \quad (11)$$

Where R_x is the logarithm of the NGD sensitivity to the specific compound and R_n, R_{n+1} are the logarithm of the NGD sensitivity to the adjacent alkanes.

To get accurate results, it is necessary to introduce simultaneously the studied compounds and the alkanes in the GC-NGD-FID instrument. Thus, a mixture of propyl to hexyl benzene and C_{10} to C_{14} (all at 10 $g.L^{-1}$ in C_5) was analyzed in isothermal conditions (T_{oven} = 90°C and T_{NGD} = 130°C). Isotherm of each analyte was plotted for three different runs (Fig. 7) and a good repeatability was demonstrated with a relative standard deviation (RSD) lower than 3% for the NGD sensitivity. In addition, based on alkanes observed in the same chromatographic run, alkylbenzenes relative response index I_R was calculated from each run. RSD values for the relative response index were lower than 0.3% for each alkylbenzene.

In some cases with the chromatographic column used, it was impossible to obtain a chromatographic separation of all compounds in a mixture of alkanes and other solutes. In such situation, the isotherms cannot be built from a data set obtained in a single run. Therefore, alkanes and ketones were injected separately, and data sets were treated independently to evaluate I_R. From these

independent injections, the RSD of relative response factor was slightly higher compared to the RSD obtained in a single run, but was still lower than 0.9%. For ketones and methyl esters, relative response factors have been obtained from independent runs and data are reported in Table 1.

Table 1: I_R results for different compounds at T_{NGD} = 130°C form separated runs (mean SD I_R = 10)

Compound	I_R	Compound	I_R
Pentan-2-one	800	Methyl octanoate	1191
Hexan-2-one	902	Methyl nonanoate	1295
Heptan-2-one	1003	Methyl decanoate	1400
Octan-2-one	1105	Methyl undecanoate	1505
Nonan-2-one	1206	Methyl dodecanoate	1609
Decan-2-one	1308		

As previously observed for alkane family, each CH_2 added in the alkly chain led to an increase of 100 in the relative response factor for alklybenzenes, ketones and fatty acid methyl esters.

4. Conclusion

This work demonstrates that in-line detection between a gas sensor (NGD) and FID was an effective way to study the interactions of a specific compound in a gaseous phase with a sensor solid phase. The equilibrium process was fully described by plotting the isotherm m_{ads}=f (C_m) from both FID and NGD response. For the NGD, the absorbed amount was not simply proportional to the concentration in the gaseous phase and Langmuir model was used to fit the data. According to thermodynamic laws, the response factor of alkanes was dependent on the number of carbon atoms in the linear alkyl chain, and inversely proportional to the absolute temperature. The sensitivity of different compounds (alkylbenzenes, ketones and esters) was compared to alkanes and a relative response factor was introduced for easier quantification of volatile organic compounds.

Using a GC instrument with an appropriate separation column, several isotherms can be obtained in a single chromatographic run, so the global methodology appears to be labor saving and time effective. As long as the sensor is not destructive and have a response time lower than the residential time of the compounds in the detectors, this GC-Sensor-FID design can be implemented for sensor response characterization.

Acknowledgment

ANTELIA and CJ Lab have provided analytical GC instrument, and Marwa CHARAF and Alex ABELLO have performed preliminary experiments using NGD detector.

References

[1] M. a. Monsoor, A. Proctor, Volatile Component Analysis of Commercially Milled Head and Broken Rice, J. Food Sci. 69 (2004) C632–C636. https://doi.org/10.1111/j.1365-2621.2004.tb09911.x.

[2] M. Moufid, B. Bouchikhi, C. Tiebe, M. Bartholmai, N. El Bari, Assessment of outdoor odor emissions from polluted sites using simultaneous thermal desorption-gas chromatography-mass spectrometry (TD-GC-MS), electronic nose in conjunction with advanced multivariate statistical approaches, Atmos. Environ. 256 (2021) 118449. https://doi.org/10.1016/j.atmosenv.2021.118449.

[3] D.M. Ruszkiewicz, D. Sanders, R. O'Brien, F. Hempel, M.J. Reed, A.C. Riepe, K. Bailie, E. Brodrick, K. Darnley, R. Ellerkmann, O. Mueller, A. Skarysz, M. Truss, T. Wortelmann, S. Yordanov, C.L.P. Thomas, B. Schaaf, M. Eddleston, Diagnosis of COVID-19 by analysis of breath with gas chromatography-ion mobility spectrometry - a feasibility study, EClinicalMedicine. 29–30 (2020) 100609. https://doi.org/10.1016/j.eclinm.2020.100609.

[4] B.P. Regmi, M. Agah, Micro Gas Chromatography: An Overview of Critical Components and Their Integration, Anal. Chem. 90 (2018) 13133–13150. https://doi.org/10.1021/acs.analchem.8b01461.

[5] G. Gregis, J.-B. Sanchez, I. Bezverkhyy, W. Guy, F. Berger, V. Fierro, J.-P. Bellat, A. Celzard, Detection and quantification of lung cancer biomarkers by a micro-analytical device using a single metal oxide-based gas sensor, Sens. Actuators B Chem. 255 (2018) 391–400. https://doi.org/10.1016/j.snb.2017.08.056.

[6] O. Martin, V. Gouttenoire, P. Villard, J. Arcamone, M. Petitjean, G. Billiot, J. Philippe, P. Puget, P. Andreucci, F. Ricoul, C. Dupré, L. Duraffourg, A. Bellemin-Comte, E. Ollier, E. Colinet, T. Ernst, Modeling and design of a fully integrated gas analyzer using a µGC and NEMS sensors, Sens. Actuators B Chem. 194 (2014) 220–228. https://doi.org/10.1016/j.snb.2013.12.075.

[7] S.K. Kim, H. Chang, E.T. Zellers, Microfabricated Gas Chromatograph for the Selective Determination of Trichloroethylene Vapor at Sub-Parts-Per-Billion Concentrations in Complex Mixtures, Anal. Chem. 83 (2011) 7198–7206. https://doi.org/10.1021/ac201788q.

[8] J. Hu, H. Qu, W. Pang, X. Duan, In-Line Detection with Microfluidic Bulk Acoustic Wave Resonator Gas Sensor for Gas Chromatography, Sensors. 21 (2021) 6800. https://doi.org/10.3390/s21206800.

[9] Y. Qin, Y.B. Gianchandani, A fully electronic microfabricated gas chromatograph with complementary capacitive detectors for indoor pollutants, Microsyst. Nanoeng. 2 (2016) 1–11. https://doi.org/10.1038/micronano.2015.49.

[10] L. Alonso Sobrado, M. Loriau, S. Junca, C. Tremaudant, P. Puget, E. Colinet, J. Randon, Characterization of Nano-Gravimetric-Detector Response and Application to Petroleum Fluids up to C34, Anal. Chem. 92 (2020) 15845–15853. https://doi.org/10.1021/acs.analchem.0c03157.

[11] R. Zhou, S. Vaihinger, K.E. Geckeler, W. Göpel, Reliable CO2 sensors with silicon-based polymers on quartz microbalance transducers, Sens. Actuators B Chem. 19 (1994) 415–420. https://doi.org/10.1016/0925-4005(93)01018-Y.

[12] P. Siciliano, Preparation, characterisation and applications of thin films for gas sensors prepared by cheap chemical method, Sens. Actuators B Chem. 70 (2000) 153–164. https://doi.org/10.1016/S0925-4005(00)00585-2.

[13] C. Zhang, S. Kaluvan, H. Zhang, G. Wang, L. Zuo, A study on the Langmuir adsorption for quartz crystal resonator based low pressure CO2 gas sensor, Measurement. 124 (2018) 286–290. https://doi.org/10.1016/j.measurement.2018.04.046.

[14] M. Akbar, H. Shakeel, M. Agah, GC-on-chip: integrated column and photoionization detector, Lab. Chip. 15 (2015) 1748–1758. https://doi.org/10.1039/C4LC01461H.

[15] S. Narayanan, G. Rice, M. Agah, A micro-discharge photoionization detector for micro-gas chromatography, Microchim. Acta. 181 (2014) 493–499. https://doi.org/10.1007/s00604-013-1146-9.

[16] G.S. Kulkarni, K. Reddy, Z. Zhong, X. Fan, Graphene nanoelectronic heterodyne sensor for rapid and sensitive vapour detection, Nat. Commun. 5 (2014) 4376. https://doi.org/10.1038/ncomms5376.

[17] I. Langmuir, THE ADSORPTION OF GASES ON PLANE SURFACES OF GLASS, MICA AND PLATINUM., J. Am. Chem. Soc. 40 (1918) 1361–1403. https://doi.org/10.1021/ja02242a004.

Figures caption

Fig. 1. Instrumental setup of the GC-NGD-FID instrument

Fig. 2. Isotherm construction methodology. (A) NGD and FID chromatograms recorded during the same analysis of a C_{10}-C_{14} mixture (10 $g.L^{-1}$), split flow = 45 $mL.min^{-1}$, pressure (He) = 1 bar, oven temperature = 110°C, NGD temperature = 130°C. (B) Normalized C_{14} signals to the highest peak in each chromatogram. (C) C_{14} adsorption isotherm (+) experimental points, red line fitted Langmuir model.

Fig. 3. (A) C_{10} to C_{14} isotherms (black cross correspond to the experimental point and red line to the model). (B) Logarithm of NGD sensitivity obtained via the isotherms of alkanes mixtures versus the number of carbon atoms. Separation Conditions: split flow = 45 $mL.min^{-1}$, pressure (He) = 1 bar, oven temperature variable, NGD temperature = 130°C.

Fig. 4. NGD and FID chromatograms of C_{14} at different NGD temperatures with the corresponding isotherms (each color corresponds to a single run with different NGD temperature). Separation Conditions: split flow = 45 $mL.min^{-1}$, pressure (He) = 1 bar, oven temperature = 110°C, NGD temperature varies from 70°C to 150°C.

Fig. 5. Logarithm of the NGD sensitivity, obtained via the isotherms of C_{10} to C_{14}, versus inverse of temperature (1/T).

Fig. 6. Logarithm of the NGD sensitivity for several compounds as a function of the number of carbon atoms. The black arrow connects different compounds with similar Ln ($Mm.K_T$) values with the hypothetical alkane having the same Ln ($Mm.K_T$) value.

Fig. 7. Isotherms of C_{10} to C_{14} and propyl to hexyl benzene of three runs at T_{NGD} = 130°C. I_R for alkylbenzenes, standard deviation (SD).

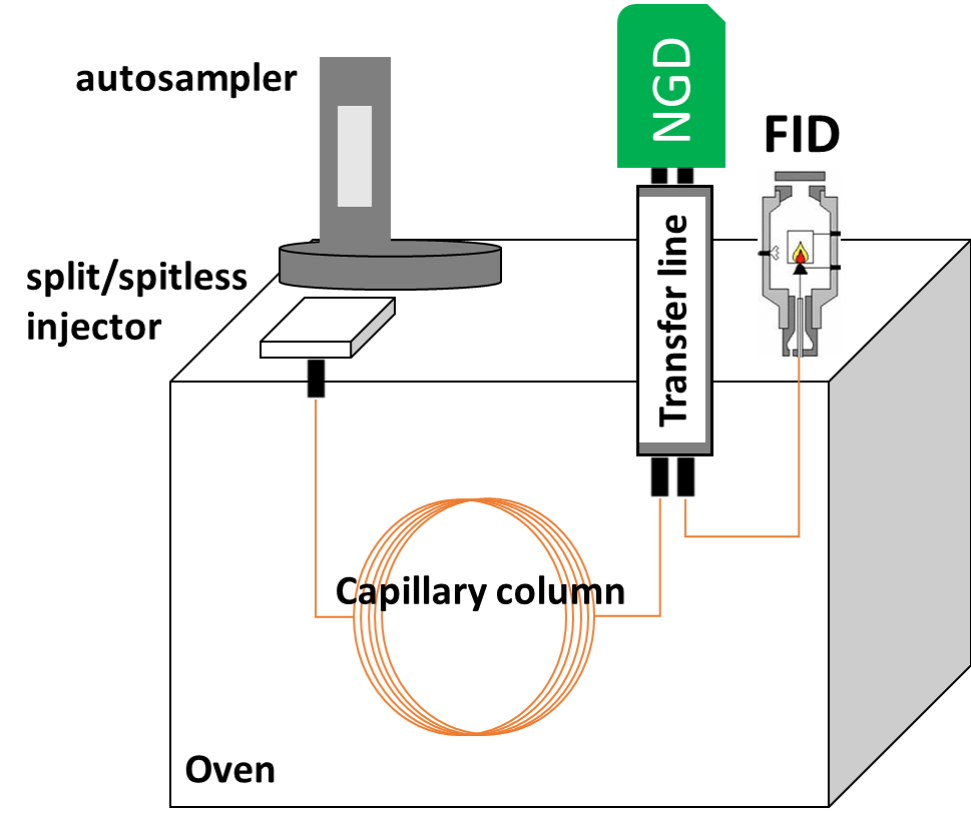
autosampler
NGD
FID
split/spitless
injector
Transfer line
Capillary column
Oven

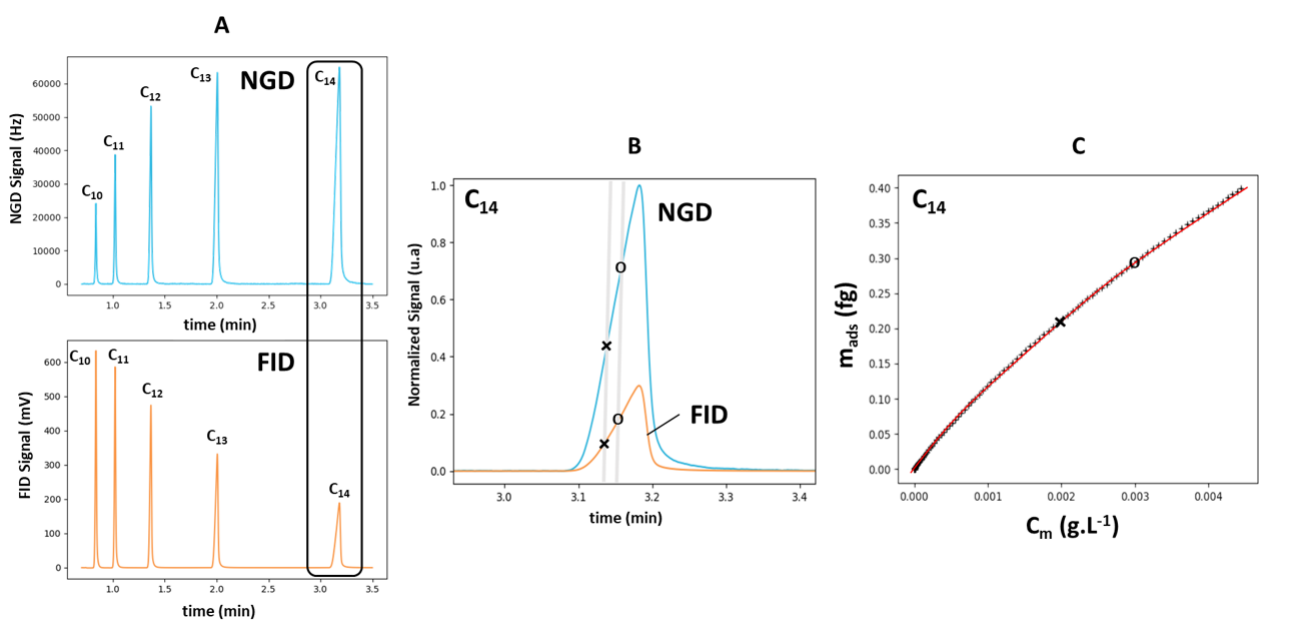
A
NGD
FID
C10
C11
C12
C13
C14
NGD Signal (Hz)
FID Signal (mV)
time (min)
B
C14
NGD
FID
Normalized Signal (u.a)
time (min)
C
C14
mads (fg)
Cm (g.L-1)

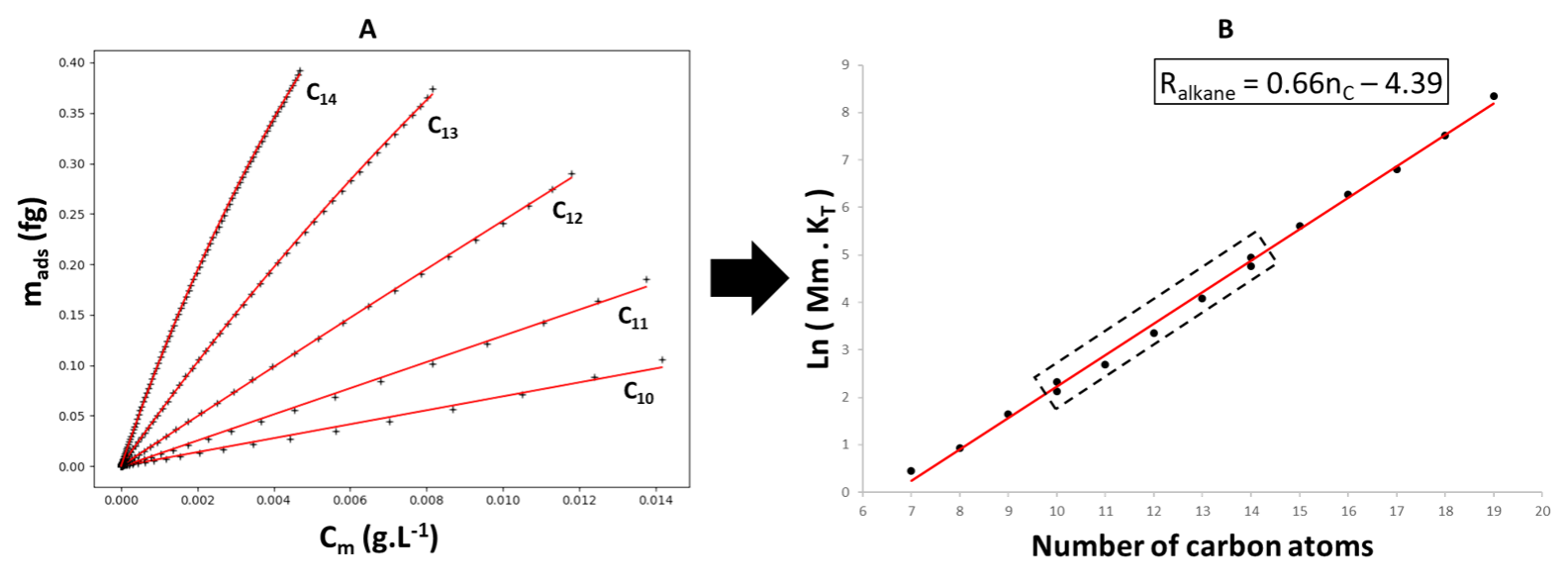
A
B
m_{ads} (fg)
C_m (g.L^{-1})
C_{14}
C_{13}
C_{12}
C_{11}
C_{10}
0.40
0.35
0.30
0.25
0.20
0.15
0.10
0.05
0.00
0.000
0.002
0.004
0.006
0.008
0.010
0.012
0.014
$R_{alkane} = 0.66n_C - 4.39$
Ln (Mm . K_T)
Number of carbon atoms
9
8
7
6
5
4
3
2
1
0
6
7
8
9
10
11
12
13
14
15
16
17
18
19
20

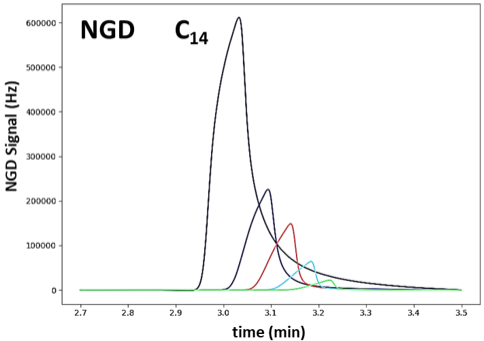
NGD
C14
NGD Signal (Hz)
time (min)

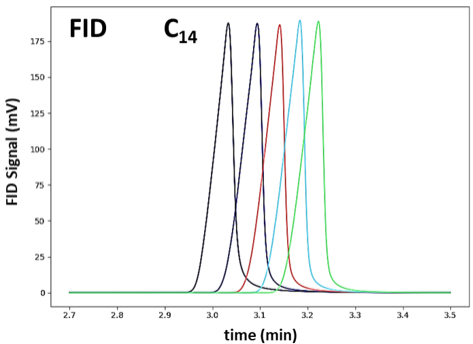
FID
C14
FID Signal (mV)
time (min)

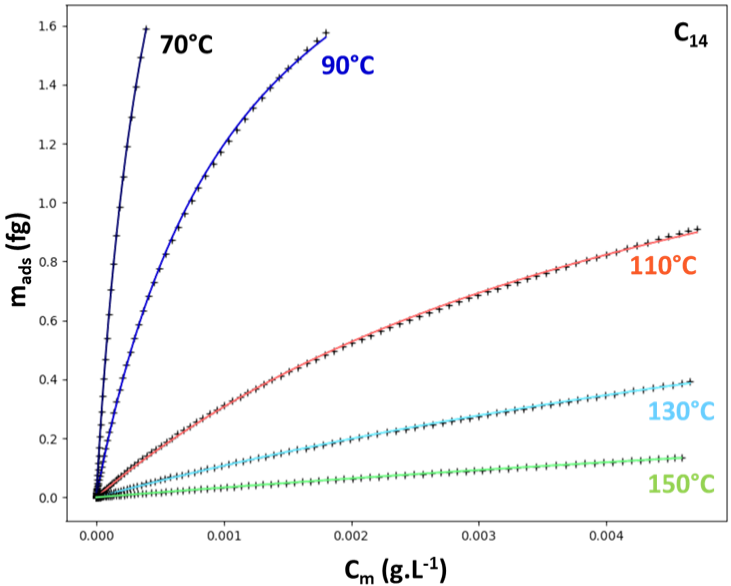
70°C
90°C
C14
110°C
130°C
150°C
mads (fg)
Cm (g.L-1)

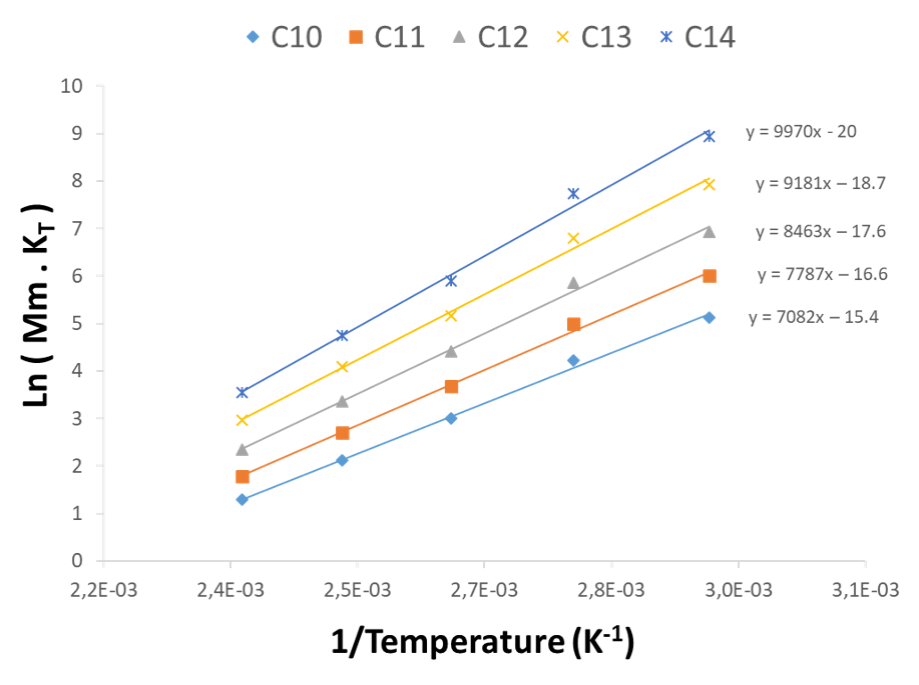
C10
C11
C12
C13
C14
y = 9970x - 20
y = 9181x – 18.7
y = 8463x – 17.6
y = 7787x – 16.6
y = 7082x – 15.4
Ln (Mm . K_T)
1/Temperature (K^-1)
10
9
8
7
6
5
4
3
2
1
0
2,2E-03
2,4E-03
2,5E-03
2,7E-03
2,8E-03
3,0E-03
3,1E-03

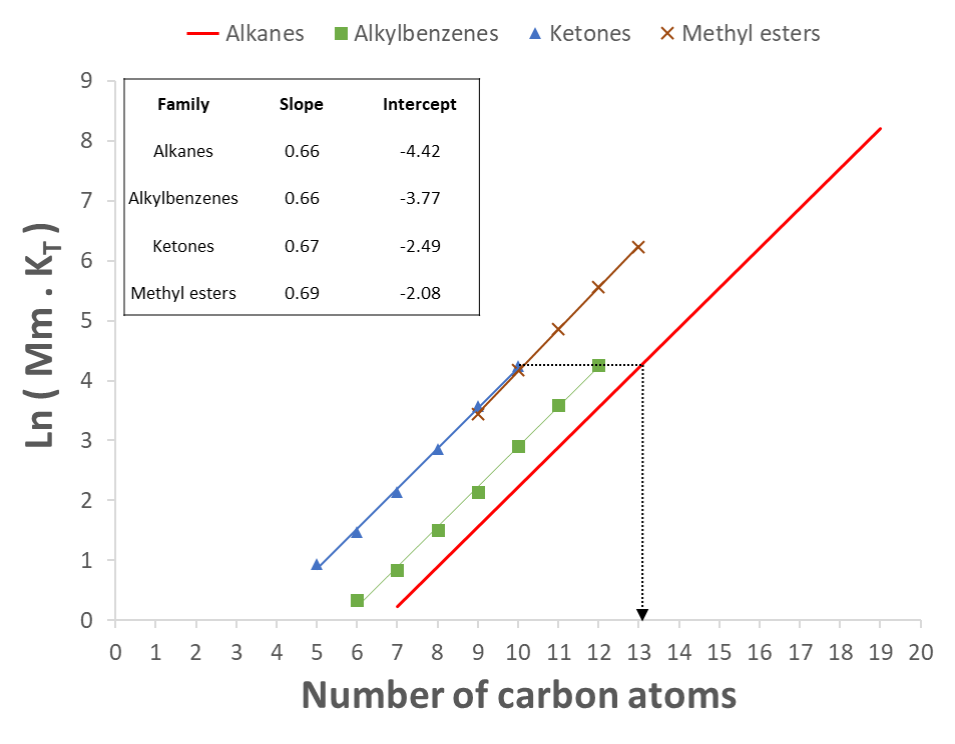
Alkanes
Alkylbenzenes
Ketones
Methyl esters
Family | Slope | Intercept
Alkanes | 0.66 | -4.42
Alkylbenzenes | 0.66 | -3.77
Ketones | 0.67 | -2.49
Methyl esters | 0.69 | -2.08
Ln (Mm . K_T)
Number of carbon atoms
0 1 2 3 4 5 6 7 8 9
0 1 2 3 4 5 6 7 8 9 10 11 12 13 14 15 16 17 18 19 20

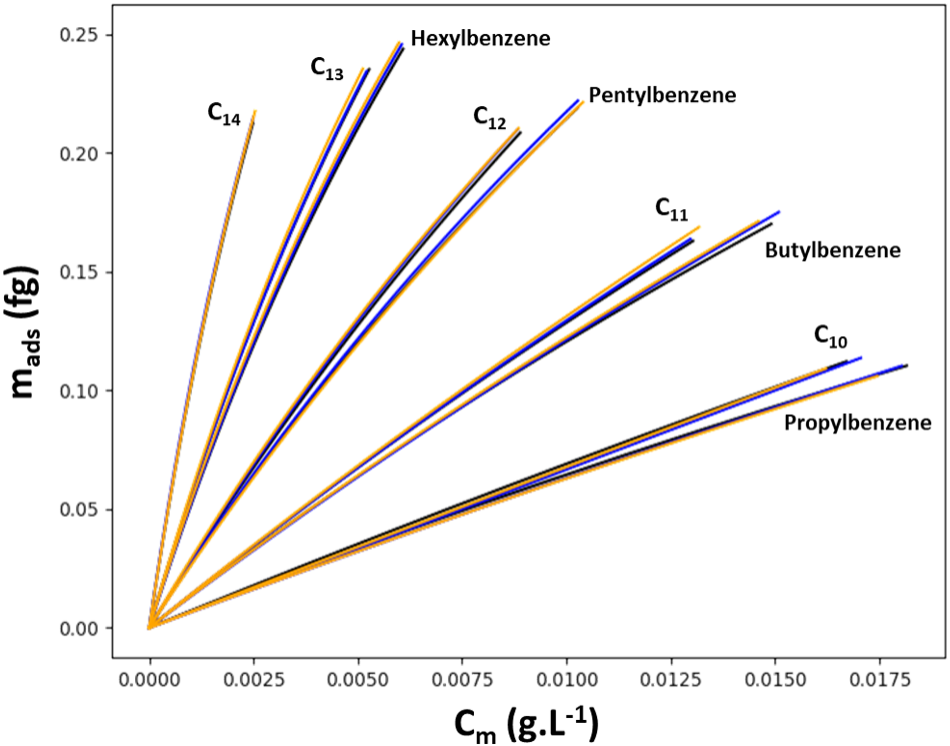

Compound	I_R ± SD
Propylbenzene	986 ± 0.3
Butylbenzene	1088 ± 1.0
Pentylbenzene	1187 ± 3.1
Hexylbenzene	1289 ± 3.7

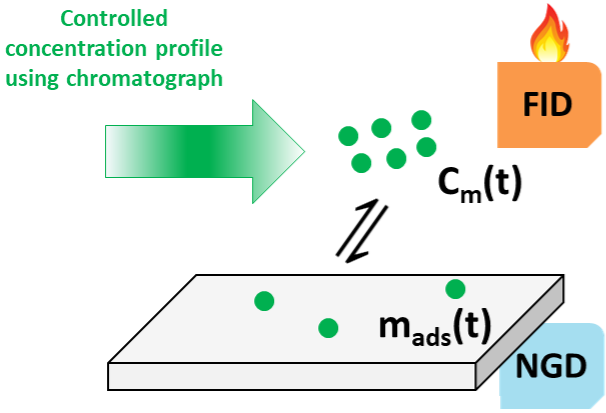
Controlled
concentration profile
using chromatograph
FID
$C_m(t)$
$m_{ads}(t)$
NGD

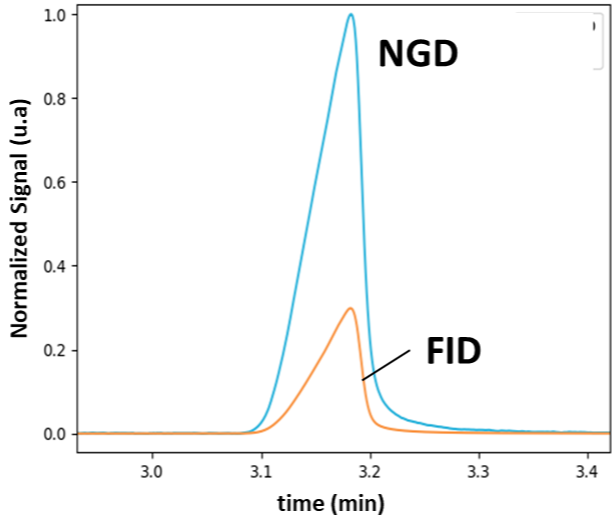
NGD
FID
Normalized Signal (u.a)
time (min)
1.0
0.8
0.6
0.4
0.2
0.0
3.0
3.1
3.2
3.3
3.4

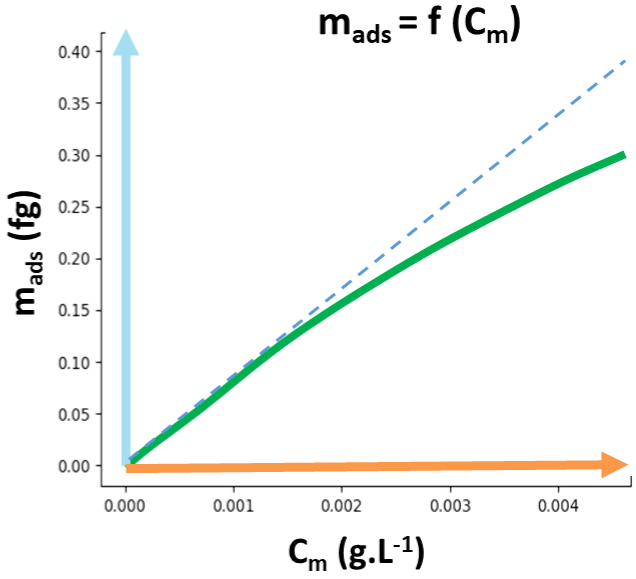
$m_{ads} = f(C_m)$
m_{ads} (fg)
C_m (g.L^{-1})
0.40
0.35
0.30
0.25
0.20
0.15
0.10
0.05
0.00
0.000
0.001
0.002
0.003
0.004